Two-Stage Kinetics of Single-Chain Collapse. Polystyrene in Cyclohexane†

Benjamin Chu* and Qicong Ying

Department of Chemistry, State University of New York at Stony Brook, Long Island, New York 11794-3400

Alexander Yu. Grosberg

Institute of Chemical Physics, Russian Academy of Sciences, 117977 Moscow, Russia

Received June 10, 1994; Revised Manuscript Received September 26, 1994®

ABSTRACT: Two-stage kinetics of single-chain collapse was clearly observed by using a thinnest capillary-tube cell with a wall thickness of 0.01 mm and a diameter of 5 mm for dynamic light scattering (DLS) measurements. Two relaxation times, τ_{crum} for the crumpled globule state and τ_{eq} for the compact globule state, were determined for the first time. Experimental DLS data measured in the coil-to-globule transition were compared with theoretical predictions.

Introduction

In considering the net attraction between parts of a single polymer molecule, Stockmayer[1] in 1960 first predicted the collapse of a polymer chain from a coil to a rather dense form. The phenomenon has attracted a great deal of attention in the past 30 years, with extensive literature on both theoretical[2−4] and experimental[5,6] aspects of this transition . The coil collapse problem is of interest not only because of biological applications such as protein folding[7] but also because of its fundamental importance as related to polymer nanostructures and fractionation. Unfortunately, it is extremely difficult to observe the coil-to-globule transition because at finite concentrations in a poor solvent, the macromolecules tend to undergo phase separation (and fractionation) when the collapsed state is being achieved. Hence, the coil collapse experiment can be classified as one of the more difficult experimental challenges among the many unsolved polymer physics problems. The first of the present authors has been working on this interesting topic since the late 1970s. Indeed, the development can be divided into several stages.[5] In the mid-1980s, a two-stage kinetics of a single-chain collapse was proposed theoretically.[8,9] The theory predicted a rather fast crumpling of the unknotted polymer chain (crumpled globule) and a subsequent slow knotting[9] or rearrangement of thermal blobs[8] of the collapsed polymer chain (compact globule). In 1992, the first successful experimental observation of a two-stage coil-to-globule transition was observed by quenching a dilute solution of polystyrene in cyclohexane just below its phase separation temperature.[10] An abrupt temperature change, from 35 to 29 °C, was employed to induce the transition from a Θ coil to a collapsed compact globule. The change in the hydrodynamic radius with time clearly exhibited the existence of a two-stage process. However, only the second stage of transition from a crumpled globule to a compact globule was observed because the first stage of transition from a Θ coil to a crumpled globule was too fast for the experimental setup at the time. The more recent computation on the coil-to-globule transition[11−15,22] has prompted further experimental tests on this interesting phenomenon.

In this work we present our recent light−scattering studies on the two-stage kinetics of polystyrene single-chain collapse in cyclohexane solution. By using a thinnest possible capillary cell in order to reduce the heat capacity of the sample chamber, the time decay of the first transition stage could be estimated. The experimental results are compared with the theoretical predictions.

Experimental Section

Materials and Sample Preparation. A polystyrene (PS) sample with a high nominal weight-average molecular weight M_w of 8.0×10^6 and a narrow molecular weight distribution M_w/M_n of 1.1 was purchased from Polymer Laboratories. It was characterized in refs 10 and 16 showing $M_w = 8.12 \times 10^6$ and $M_z/M_w = 1.08$. Both the value of M_w/M_n and that of M_z/M_w confirmed this sample to have a fairly narrow molecular weight distribution. The solvent HPLC-grade cyclohexane (CYH) was purchased from Aldrich Chemical Co. It was dried by using 4-Å molecular sieve beads, which was activated at 400 °C for 2 h, distilled in the presence of additional newly activated 4-Å molecular sieve beads, and stored in a drybox before use. The preparation of a dust-free solution for dynamic light scattering (DLS) measurements has been described previously.[10] A dilute concentration of 8.70×10^{-6} g/mL of a PS−CYH solution was used for DLS measurements.

DLS Measurements. DLS measurements were conducted by using a conventional laser light-scattering spectrometer operating at a wavelength of 514.5 nm.[17] The polymer solution was quenched to a designated temperature from the Θ temperature (35 °C) in order to induce the macromolecular size change, which was determined by means of DLS in terms of the hydrodynamic radius (R_h).

Measurements of the intensity autocorrelation function $G^{(2)}(\tau)$ were made at a scattering angle of 33°. The unnormalized intensity autocorrelation function $G^{(2)}(\tau)$ has the form

$$G^{(2)}(\tau) = A[1 + \beta|g^{(1)}(\tau)|^2] \quad (1)$$

with τ ($\equiv\Gamma^{-1}$) being the delay time, A the base line, β a spatial coherence factor, and $g^{(1)}(\tau)$ the first-order normalized electric field time correlation function, which is related to the normalized characteristic line-width distribution function $G(\Gamma)$ by the Laplace transformation:

$$g^{(1)}(\tau) = \int G(\Gamma) \exp(-\Gamma\tau)\, d\Gamma \quad (2)$$

* Author to whom all correspondence should be addressed.

† Presented at the symposium in honor of Walter H. Stockmayer on his 80th birthday, at the ACS meeting in San Diego.

® Abstract published in *Advance ACS Abstracts,* November 15, 1994.

0024-9297/95/2228-0180$09.00/0

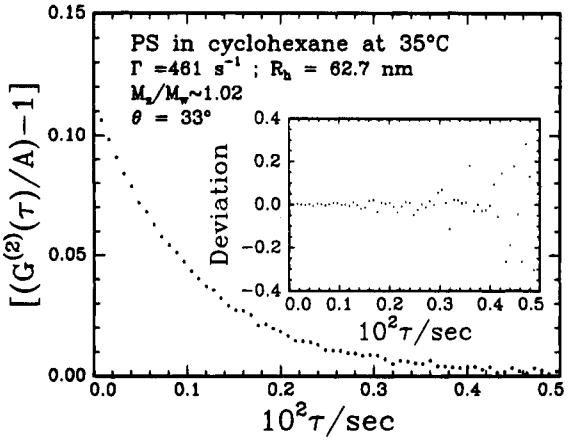

Figure 1. Normalized intensity autocorrelation data of PS in cyclohexane with $\bar{\Gamma} = 461\ s^{-1}$ and variance $\mu_2/\bar{\Gamma}^2 \simeq 0.004$ measured at a Θ temperature of 35.0 °C and $\Theta = 33°$, R_h = 62.7 nm, and $M_z/M_w = 1.02$. The inset shows the deviation plot based on the second-order cumulants fit.

Data analysis of the electric field time correlation curve was performed by using the method of cumulants[18] and the CONTIN method,[19] yielding an average line width $\bar{\Gamma}$ and the variance $\mu_2/\bar{\Gamma}^2$, with

$$\bar{\Gamma} = \int \Gamma G(\Gamma)\, d\Gamma \tag{3}$$

and

$$\mu_2 = \int (\Gamma - \bar{\Gamma})^2 G(\Gamma)\, d\Gamma \tag{4}$$

In the CONTIN method, one can analyze the data by using either $\bar{\Gamma}$ or $\tau(\equiv\bar{\Gamma}^{-1})$ as the variable. The results are weighted differently, yielding slightly different numerical values for R_h. In the limit of $qR_g < 1$ and at very dilute solution concentrations, $\bar{\Gamma} = D_z q^2$, where D_z is the z-average translational diffusion coefficient. According to the Stokes–Einstein relation, $R_h = k_B T/(6\pi\eta D)$, with k_B being the Boltzmann constant, T the temperature (K), and η the solvent viscosity in Poise. The size distribution based on the hydrodynamic radius for the collapsed globule was evaluated by using the CONTIN method.[19] Figure 1 shows the normalized intensity autocorrelation data of a PS–CYH solution with $\bar{\Gamma} = 461\ s^{-1}$ and $\mu_2/\bar{\Gamma}^2 \simeq 0.004$ at a Θ temperature of 35 °C and a scattering angle of 33° (where, for our sample, the value of $qR_{g,\Theta}(\simeq 0.85) < 1$), yielding R_h = 62.7 nm and $M_z/M_w \cong 1.02$, respectively. We used the relation $M_z/M_w = 1 + 4(\mu_2/\bar{\Gamma}^2)$ to estimate the polydispersity effect.[20] The results are in good agreement with that presented in ref 10 within the experimental error limits.

When a polymer solution was quenched from the homogeneous one-phase region to an unstable or metastable two-phase region, the collapse of single chains due to intramolecular interactions is in time competition with the intermolecular aggregation of polymer chains. Hence, the time for the polymer solution to reach the new designated temperature in a quenching process is an important factor that may determine whether the kinetics of coil collapse can be observed experimentally. To shorten the thermal equilibration time to a predesignated constant temperature without drastic mechanical changes in the light-scattering spectrometer, attempts were made to reduce the heat capacity of the sample cell. Three different types of scattering cells were used in the present study: cell A was made from an optical glass tubing with a diameter (d) of 10 mm and a wall thickness (δ) of 1.0 mm; cell B with d = 10 mm and δ = 0.3 mm; and cell C with d = 5 mm and δ = 0.01 mm. A small thermistor was inserted into the cell filled with solvent for simulation of the temperature changes in the quenching process. Figure 2 shows the temperature–time curves of the three different cells by quenching the cells from 35.0 to 28.0 °C, which was one of the designated temperatures for the coil-to-globule transition

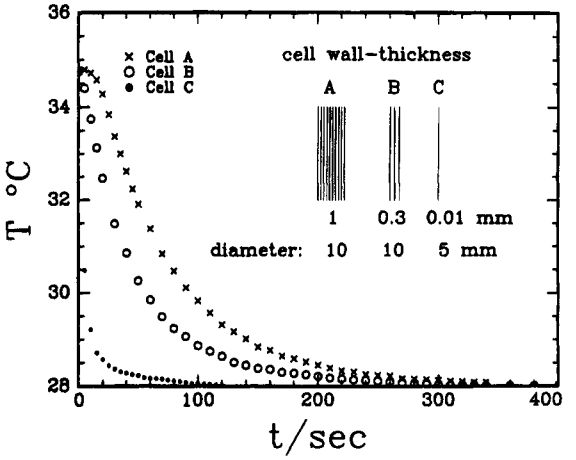

Figure 2. Temperature–time curves for different light scattering cells used in the quenching process. t is the time after quenching the light-scattering cell from 35.0 to 28.0 °C. Crosses denote cell A with diameter d = 10 mm and wall thickness δ = 1 mm; hollow circles, cell B with d = 10 mm and δ = 0.3 mm; filled circles, capillary cell C with d = 5 mm and δ = 0.01 mm.

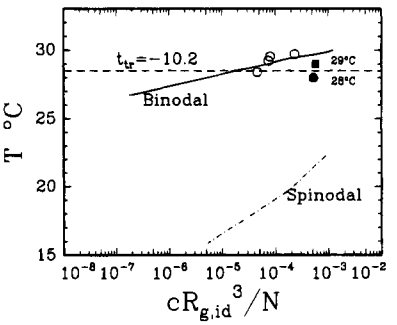

Figure 3. Phase diagram of the PS–CYH system. The solid line and dot-dashed line are theoretical binodal and spinodal curves.[11] The dashed line denotes the coil-to-globule transition point, where the reduced transition temperature $t = t_{tr} = -10.2$. Hollow circles denote the concentration regime in ref 21. Filled symbols denote the present work with $c = 5.04 \times 10^{16}$ link/cm^3, $R_{g,id} = 9.32 \times 10^{-6}$ cm, and $N = 7.81 \times 10^4$.

measurements in the present work. The experimentally measured thermal equilibration time for the thinnest capillary-tube cell was around 80 s, which was much shorter than that for the other two cells.

Results and Discussion

I. Two-Stage Coil-to-Globule Transition. The coil-to-globule transition of a PS–CYH solution was carefully investigated at a quenched final temperature of 28.0 °C, somewhat below the coil-to-globule transition temperature of 28.5 °C, as estimated by Grosberg and Kuznetsov for the PS–CYH system of the given molecular weight.[11] The PS–CYH solution at a concentration of 8.70×10^{-6} g/mL and 28.0 °C represented an experimental condition in the metastable region (filled circle) as shown in Figure 3. The hollow circles denote the experimental region reported in ref 21 where the coil-to-globule transition was studied by means of viscosimetry. The filled square denotes the DLS measurements[10] for quenching the PS–CYH system from 35 to 29 °C and the filled circle those from 35 to 28 °C. The solid line and the dot-dashed line respectively are the theoretical binodal and spinodal curves.[11] According to the theory,[11] a reduced temperature (see eq 7 below) t_{tr} of −10.2 represents the coil-to-globule transition range (dashed line), which corresponds to 28.5 °C for the PS–CYH system with $M = 8 \times 10^6$. After the PS–CYH

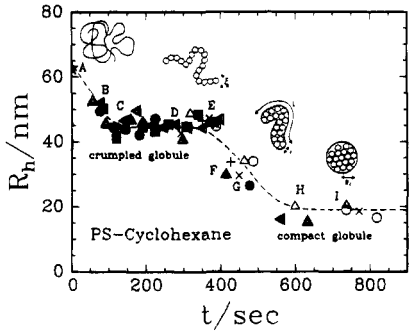

Figure 4. Time dependence of the hydrodynamic radius of a single polystyrene chain in cyclohexane. The sample was quenched from 35.0 to 28.0 °C at a concentration of 8.70×10^{-6} g/mL and a scattering angle of 33°. Filled symbols denote data measured by using capillary cells. Hollow circles and triangles denote data measured by using cells with $d = 10$ mm and $\delta = 1$ mm. Crosses and pluses denote data measured by using cells with $d = 10$ mm and $\delta = 0.3$ mm. The dashed line is for guiding the eyes. The filled star (A) denotes the original sample measured at 35.0 °C. Positions B, C, D, E, F, G, H, and I denote the measurement times at 85, 125, 271, 372, 414, 477, 611, and 737 s, respectively, after quenching the sample from 35.0 to 28.0 °C. Pictures were copied from Figure 1 in ref 8.

solution was quenched from 35.0 to 28.0 °C, the time dependence of the hydrodynamic size of PS macromolecules in cyclohexane measured by using different light-scattering cells is shown in Figure 4.

The filled symbols denote the data measured by using the thinnest capillary cells with $d = 5$ mm and $\delta = 0.01$ mm. Pluses/crosses and hollow symbols are the data measured by using cells with $d = 10$ mm and $\delta = 0.3$ mm and 1 mm, respectively. As has been shown in the previous work,[10] the transition from the crumpled globule to the compact globule could be observed by using those thick-walled cells, but the time effect on the first transition from an ideal Θ coil to the crumpled globule could not be established because of the long thermal equilibration time required by those thick-walled and larger diameter cells. The details of the kinetic transition from the Θ coil to the crumpled globule could be explored only by using the thinnest capillary cells.

According to the theoretical work,[8,9] the conformation of a macromolecular chain in the coil-to-globule transition could be modeled as a Θ coil in the initial stage and as a compact sphere in the final stage. However, in the intermediate range, the conformation of a macromolecular chain could perhaps exist as a "sausage"-like chain as proposed by de Gennes[8] and shown schematically in Figure 4 and, at a later intermediate stage, a "crumpled globule" as predicted in ref 9.

During the coil-to-globule transition process, the time dependence of the normalized intensity autocorrelation function, determined at different stages of collapse, is exhibited in Figures 5–9, with the changes in the corresponding hydrodynamic radius R_h distribution shown in the insets, where $W(R_h)$ denotes the weight fraction at R_h. It should be noted that the interpretation of the following experimental results (Figures 4–9) is independent of the theoretical models but represents mainly the experimental observations.

In parts a and b of Figure 5, the intensity time autocorrelation functions were measured at times $t =$ 85 and 125 s (positions B and C in Figure 4), respectively, after the PS–CYH solution was quenched from 35.0 to 28.0 °C. In the first transition stage, the shape

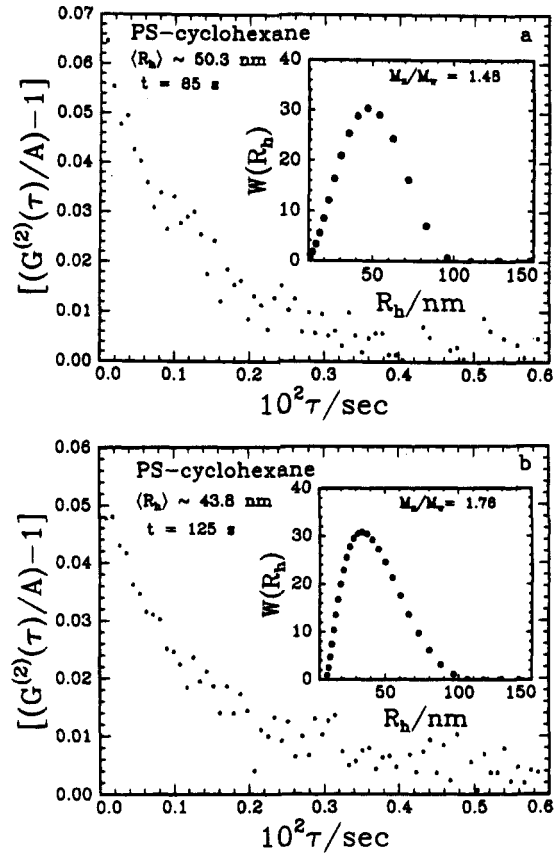

Figure 5. Normalized intensity autocorrelation data and distribution of the hydrodynamic radius, from the CONTIN analysis, of globules of PS in cyclohexane, as determined at different measurement times after the sample was quenched from 35.0 to 28.0 °C: (a) 85 s (position B in Figure 4); (b) 125 s (position C in Figure 4).

of R_h distributions still obeyed a single-modal distribution, but the polydispersity of R_h distributions (M_z/M_w) changed with time, from 1.02 (Θ coil, position A in Figure 4) to 1.48 (position B) and then to 1.76 (position C), where the symmetrical shape of the distribution curve began to be distorted, with the larger size end of the distribution curve being stretched out. The experimental observation could imply that, even in the crumpled stage, the aggregation of polymer coils due to intermolecular interactions occurred, yielding an apparent larger value in terms of M_z/M_w. The smaller size aggregates did not appear as a separate entity because those sizes were sufficiently close to the single crumpled globule and DLS could not yet resolve the bimodal distribution.

The asymmetrical behavior of the R_h distribution curves, manifested clearly in parts a and b of Figure 6, was measured at 271 and 372 s, respectively (positions D and E in Figure 4), after quenching. The average size remained relatively constant with $R_h \simeq 44.7$ nm, but M_z/M_w increased from 1.76 (position C) to a value of 2.04 (position D) and then to 2.64 (position E). The fairly constant value of R_h (≃45 nm) confirms that the single coils have reached a slightly contracted size when compared with the size of a Θ coil. The increase in the variance from ~1.02 to 2.64 suggests the presence of a very small amount of aggregates which is growing in size. The CONTIN method of analysis could not resolve the bimodal distribution. This large increase in the variance also does not exclude an increase in the very small amount of the aggregates. In addition, with the $\langle R_h \rangle$ values remaining relatively constant, the large

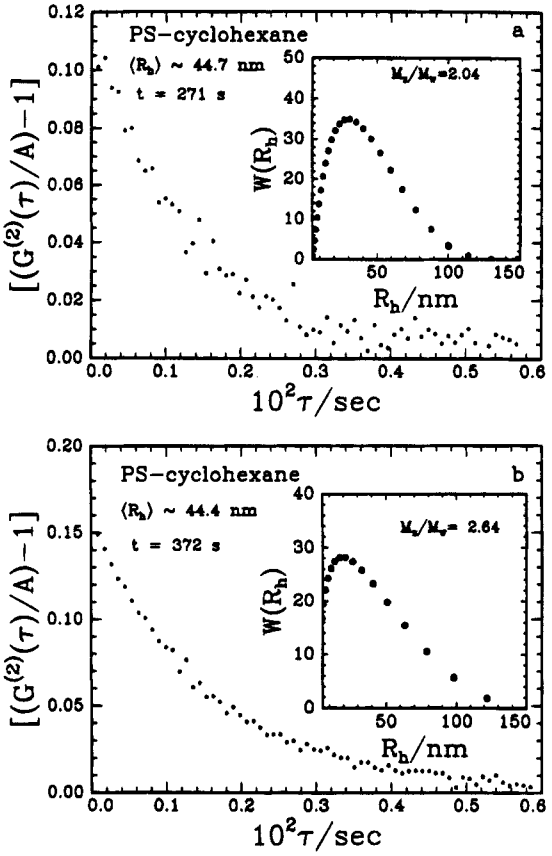

Figure 6. Normalized intensity autocorrelation data and distribution of the hydrodynamic radius, from the CONTIN analysis, of globules of PS in cyclohexane as determined at different measurement times after the sample was quenched from 35.0 to 28.0 °C: (a) 271 s (position D in Figure 4); (b) 372 s (position E in Figure 4).

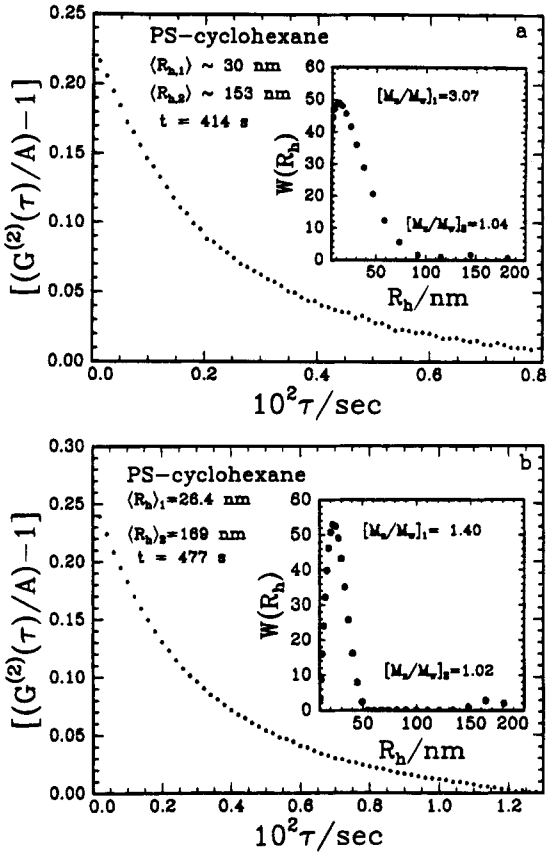

Figure 7. Normalized intensity autocorrelation data and distribution of the hydrodynamic radius, from the CONTIN analysis, of globules of PS in cyclohexane as determined at different measurement times after the sample was quenched from 35.0 to 28.0 °C: (a) 414 s (position F in Figure 4); (b) 477 s (position G in Figure 4).

increase in the variance, expressed as apparent M_z/M_w ratios, could imply that the size of the single coils is decreasing slowly. In addition, R_h for the crumpled globule represents an upper limit since it includes a contribution from the aggregates.

While the elapsed time proceeded to 414 s (position F in Figure 4), the single-chain collapsed process entered the second transition period, where the intensity time correlation function was coincidentally no longer close to a single exponential, and the size distribution began to become bimodal, as shown in Figure 7a. The small-size globules (collapsed single chains) had an average size of $R_h \simeq 30$ nm and $M_z/M_w \simeq 3.07$. This size value was much smaller than the values of 153 nm of the large-size aggregates, which had a relatively uniform distribution with M_z/M_w of 1.04. The weight fraction of the small-size globules was about 96% as calculated from the area ratio of the normalized weight distribution curve of R_h. In the middle of this transition period, where $t = 447$ s (position G in Figure 4), the collapsed single-chain shrunk further to a size $R_h \simeq 26.4$ nm with a polydispersity $M_z/M_w \simeq 1.40$. The weight fraction of the small-size globules was about 93%, as shown in Figure 7b. The small-size globules became the dominant state at the second transition stage. It should be noted that, while the single coil size was undergoing the second transition from the crumpled globule to the compact globule, the coils in the aggregates followed a similar contraction. Therefore, from parts a to b of Figure 7, even though the aggregates increased in size from 153 to 169 nm, in reality, the measured size would have been larger except for the fact that the entangled coils in the aggregates also began to contract. The entanglement could also slow down the contraction. Thus, the aggregate contraction became noticeable at a later time.

At 611 s after quenching (position H in Figure 4), the chain collapse process almost reached the compact globule state. The weight fraction of the small globules, with $R_h = 20.8$ nm and $M_z/M_w = 2.36$, still kept a value of around 92%, as shown in Figure 8a, and the size of the large-size aggregates actually decreased slightly. In the compact globule stage (position I in Figure 4), the weight fraction of the compact globules (and also the aggregated chains) started to change gradually. It is clearly shown in Figure 8b that the weight fraction of the small globules, with $R_h = 20.4$ and $M_z/M_w = 2.69$, decreased to 73% (from 92% in Figure 8a); some of the single coils could aggregate and contribute to both the small and large aggregate size fractions, yielding a smaller average $R_h = 81.3$ nm for the larger-size fraction and a broad size distribution for the small-size fraction.

Eventually, as shown in parts a and b of Figure 9, the bimodal behavior disappeared and the dominant intensity contribution came from the aggregates. The average size of the aggregates increased from 95 nm at $t = 841$ s to 149 nm at $t = 927$ s. At the same time the small-size end of the size distribution curve faded away, and the polydispersity of the aggregates decreased from 2.17 to 1.34, denoting that the aggregate size became more uniform.

From the two plateau regimes in Figure 4, the hydrodynamic radii of the PS chain at 28.0 °C were estimated to be 44.7 and 19.5 nm for the crumpled

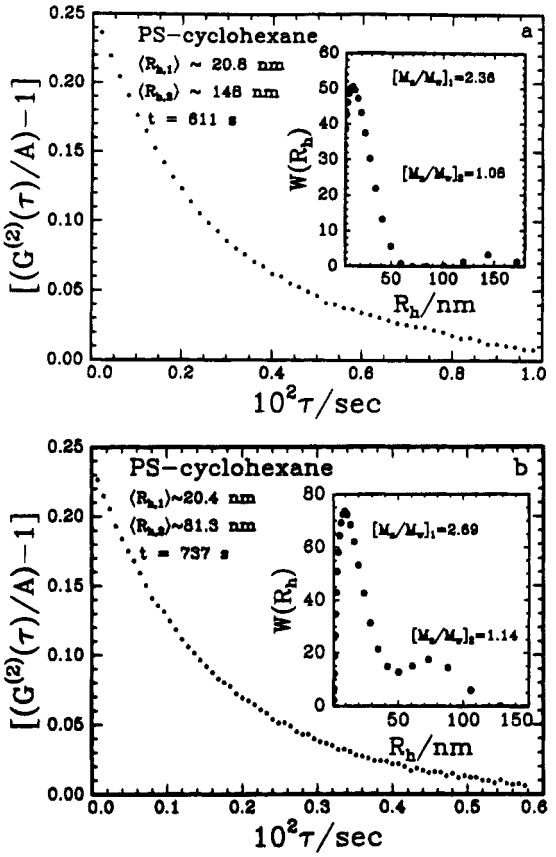

Figure 8. Normalized intensity autocorrelation data and distribution of the hydrodynamic radius, from the CONTIN analysis, of globules of PS in cyclohexane as determined at different measurement times after the sample was quenched from 35.0 to 28.0 °C: (a) 611 s (position H in Figure 4); (b) 737 s (position I in Figure 4).

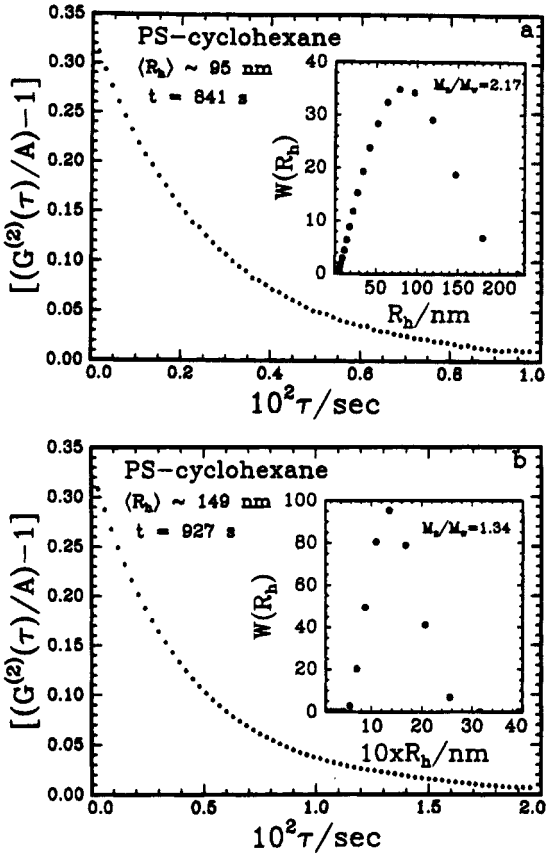

Figure 9. Normalized intensity autocorrelation data and distribution of the hydrodynamic radius, from the CONTIN analysis, of globules of PS in cyclohexane as determined at different measurement times after the sample was quenched from 35.0 to 28.0 °C: (a) 841 s; (b) 927 s.

globule and the compact globule, respectively. A master curve of the scaled expansion factor of hydrodynamic size $\alpha_h^3\tau M_w^{1/2}$ versus $\tau M_w^{1/2}$ is shown in Figure 10, where $\alpha_h = R_h(T)/R_h(\Theta)$ and $\tau = 1-(T/\Theta)$. Hollow circles denote the results determined at stable equilibrium;[4] the filled triangle and star signify the results from ref 10. The filled circles and squares denote respectively the current results from the crumpled globule and the compact globule measured at 28.0 and 29.0 °C. The expansion factors in the two plateau regimes in Figure 4 had 0.71 for the crumpled single-chain globule and 0.31 for the compact single-chain globule at 28 °C. In comparison with data determined at stable equilibrium (hollow circles in Figure 10),[4] the reduced expansion factor for the crumpled globule was close to the results measured at stable equilibrium in the homogeneous one-phase region. The reduced expansion factor for the compact globule decreased sharply and reached a globular asymptote.

II. Overview of Theoretical Models. The theory of the equilibrium globule has been developed, at least on the mean-field level (see, for example, refs 11–15). By contrast, there are only few theoretical works on the kinetics of the coil–globule transition.[8,9,23–28] The kinetic theories are either qualitative in character[8,9] or based on computer simulation techniques[23–27] which are restricted to very short chains,[24–27] or restricted to a two-dimensional system,[25] or deal with peculiar models.[23] The question is whether we can promote the understanding gained from theoretical works to interpret the experimental findings.

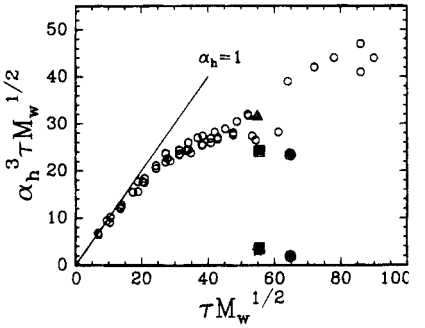

Figure 10. Plot of the master curve of $\alpha_h^3\tau M_w^{1/2}$ vs $\tau M_w^{1/2}$. Hollow circles denote the homogeneous one-phase results in ref 5. The filled triangle and star denote the results in ref 10. Filled circles and squares denote the present results determined at 28.0 and 29.0 °C, respectively.

The theory by de Gennes[8] implies that, after having sharply quenched the polymer coil to poor solvent conditions, the chain collapse takes place in a self-similar manner by gradual shortening and thickening of the sausage-like conformation as shown schematically in the inset of Figure 4. This self-similar mechanism is also revealed by an earlier computer simulation.[24] We will see below in section III that the characteristic relaxation time predicted by this theory ($\sim 10^{-3}$ s, which was estimated based on the value of the *solvent* viscosity η_0) is many orders of magnitude lower than what is observed experimentally ($\sim 10^2$ s). Therefore, the viscosity used in estimating the characteristic relaxation time should be defined differently as de Gennes speculated very briefly in ref 8.

What could be the physical nature of these very long experimentally observed relaxation times ($\sim 10^2$ s)?

One of the *possible explanations* is due to the topological constraints and self-entanglements of the globule. The role played by these factors was analyzed, on a very qualitative level, in the theory of Grosberg et al.,[9] which predicted that the collapse could be a two-stage process, with the shorter stage (called crumpling) beign almost identical to what was described by de Gennes,[8] while the longer "topological" stage was supposed to be similar to self-reptation. In section IV, we attempt to fit experimental results with this theory.

It is worthwhile to note that, while attributing the origin of the longer relaxation time to self-entanglements, one implies an important peculiar role to the chain ends, such that the dynamics of ring polymer collapse is expected to differ dramatically from the linear chain case. The role of chain ends is also stressed in the recent work by Ostrowsky and Bar-Yam.[23] It would be very interesting to examine experimentally this theoretical conjecture.

Another view on the dynamics of the coil-to-globule transition is revealed by a recent computer simulation of rather short 2D lattice chains,[25] where a two-stage process has been "observed". The first (fast) stage is a general increase of the chain density, while the second stage takes longer time because it requires partial opening, or melting, of an already very dense globule. This mechansim could be important for a coil collapse in an extremely poor solvent, where the first fast stage of collapse would already result in the formation of a very dense globule. However, in the present experiment, we have quenched from the Θ temperature at 35 °C to only 28 °C. We shall show that the volume fraction of the polymer inside the globule does not exceed 50%.

For completeness, we mention here also the recent works[26-28] on computer simulations of collapse kinetics for heteropolymers, on both 2D[27] and 3D[26,28] lattice models. The main focus of these works is to model protein folding with formation of a unique native structure. Very peculiar physics is involved in this process, such as the choice of appropriate contacts in the highly heterogeneous system. This is of course very different from the present work.

III. Comparison of the de Gennes prediction[8] with Experimental Data. In the de Gennes theory, the polymer chain at the temperature $T = \Theta - \Delta T$ is divided into "blobs" of g [$=(\Theta/\Delta T)^2$] monomers with a blob size ξ of $ag^{1/2}$, a being the monomer segment length. Thus, the size of the polymer chain scales as $R_h(\Delta T) \sim \Delta T^{-1/3}$, with ΔT being the temperature deviation from the Θ temperature. Experimentally $R_{h,comp}(28\ °C) \approx 20$ nm and $\Theta = 35$ °C. $R_{h,comp}(29\ °C) \approx R_{h,comp}(28\ °C)[7/6]^{1/3} \approx 23 \pm 3$ nm. However, this test is certainly insufficient. Further experiments with larger values of ΔT are in progress. Furthermore, from a theoretical perspective, we do not expect this $^1/_3$ scaling to be obeyed in the temperature range at hand, as it stems from the so-called volume approximation which is definitely not correct in the vicinity of the coil–globule transition temperature.

After having quenched the polymer solution from 35 to 28 °C, the original Θ coil, as shown shchematically in the left figure in Figure 4, is reduced to a string of N/g blobs, each with size ξ, as shown schematically in the second figure from the left in Figure 4. The blobs were assumed to stick together so as to minimize the surface energy between an inner domain of concentration C_g and free solvent. At the starting point, de Gennes took the sausage to have a length $L = (N/g)\xi$ and a cross-section size $r = \xi$. At later times, the sausage swells laterally and contracts longitudinally, keeping a constant volume $\Omega = \pi r^2 L$, as shown schematically in the third figure from the left in Figure 4. It should be noted that self-crossing is neglected and the model does not include knotting.

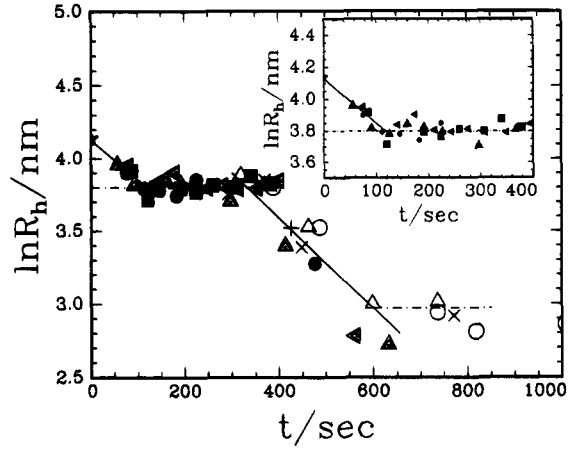

Figure 11. Semilogarithmic plot of the time dependence of the hydrodynamic radius of a single polystyrene chain in cyclohexane. The sample was quenched from 35.0 to 28.0 °C at a concentration of 8.70×10^{-6} g/mL and a scattering angle of 33.0°. Filled symbols denote data measured by using very thin-walled capillary cells. Symbols are the same as in Figure 4. Solid lines are linear fitting results. The equations of fitting lines are represented as $\ln R_h/\text{nm} = 4.13 - 0.28 \times 10^{-2} t/\text{s}$ for the crumpled stage and $\ln R_h/\text{nm} = 4.83 - 0.31 \times 10^{-2} t/\text{s}$ for the collapsed stage. Dot-dashed lines are for guiding the eyes.

According to the de Gennes model,[8] the chain radius is predicted to behave as

$$R_h(t) \simeq R_{h_{id}}[1 - t/\tau_c]^{1/5} \tag{5}$$

where τ_c is given by

$$\tau_c \sim \frac{\eta}{k_B\Theta} a^3 \frac{\Delta T}{\Theta} N^2 \tag{6}$$

with η being the solvent viscosity. With $a \sim 1$ nm, $N \sim 10^5$, $\eta = 0.834 \times 10^{-2}$ P (for CYH at 28 °C), $k_B = 1.38 \times 10^{-16}$ erg/K, $\Delta T = 7$ °C, and $\Theta = 308$ K, we get $\tau_c \sim 10^{-2}$ s. The initial sausage-type relaxation might be followed by some exponential stage of relaxation, which was not analyzed in ref 8. Figure 11 shows an experimental plot of $\ln R_h$ versus time. It was interpreted in terms of two exponents of the type $e^{-t/\tau}$ (here we have assumed $R_h(t \to \infty)$ can be decayed hypothetically to zero) with characteristic times of 357 and 323 s, respectively. The absolute value of τ is base-line dependent, but the ratio of the characteristic times remains a constant. Nevertheless, the characteristic times τ found in the present work are several orders of magnitude longer when compared with the theoretical estimate based on the de Gennes model. This huge discrepancy encourages us to speculate that yet another physical mechanism could be relevant and should be taken into account in order to understand what is observed. In this spirit, we have to address two closely related issues, i.e., the topological constraints, entanglements, and knotting in the collapsed but not fully relaxed chain and the effective viscosity η_{eff}, as experienced by a collapsing globule, which is much higher than the viscosity of pure solvent η_0.

IV. Quantitative Comparison of Mean-Field Theory Results with Our Experimental Data. As described above, the experiment with the thinnest capillary has allowed us to clearly observe a two-stage collapse process within essentially a single macromolecule. We have also discussed briefly the qualitative explanation of this two-stage kinetics. It is now a challenge to understand whether we can promote this understanding more quantitatively. We shall begin the comparison of data with theory at equilibrium conditions and then go to the kinetic study.

IV.1. Which Parameters Are Involved in the Theory? We used the same notations as in refs 11–15. The mean-field theory deals with the following parameters: the number of monomers per chain N; "monomer size" a, defined in such a way that the mean-square ideal Gaussian coil radius of gyration is equal to $R_{g,id} = aN^{1/2}$; pairwise and triple interaction constants are denoted by B and C. Let us recall that the dimensionless value of $\sqrt{C}/a^3$ is related to the chain stiffness, while another dimensionless parameter

$$t_r = 6^{3/4}BN^{1/2}C^{-1/4}a^{-3/2} \sim \frac{T-\Theta}{\Theta}N^{1/2} \qquad (7)$$

is used as the "reduced temperature". In the vicinity of the Θ-point, t_r is proportional to $\tau = (T-\Theta)/\Theta$, with T being the absolute temperature. In order to relate the theoretical predictions to the real temperature measurements, one has to introduce a parameter Q which defines the quantitative relationship between the reduced temperature t_r and the real temperature T, or τ:

$$t_r = Q\tau\sqrt{M} \qquad (8)$$

It should be noted that the chain stiffness parameter $\sqrt{C}/a^3$ defines the qualitative shape of the coil-to-globule transition as well as nearly every property of the polymer–solvent system, while Q is far less important, defining only the scale along the temperature axis. $\sqrt{C}/a^3$ was estimated to be 0.15.[11,15]

To describe the dynamic behavior, the value of the solvent viscosity η_0 and of the entanglement constant N_e should be additionally incorporated.

IV.2. Which Parameters Are Known? First, let us summarize what we consider to be the reliable numerical information concerning the PS–CYH system.

(i) With a molecular mass of $M \approx 8.12 \times 10^6$ used in the experiment, the number of monomers per one chain is about $N = M/m = 8.12 \times 10^6/104 \approx 7.81 \times 10^4$.

(ii) According to the Grosberg–Kuznetsov theory, the radius of gyration of a polymer chain at Θ conditions can be written as

$$R_{g,\Theta}{}^2 = R_{g,id}{}^2[1 - 6.668(\sqrt{C}/a^3)^2] \qquad (9)$$

with $\sqrt{C}/a^3 = 0.15$. In ref 5 the ratio of $R_{g,\Theta}/R_{h,\Theta}$ is equal to 1.37, at $\Theta = 35$ °C, as was determined for a similar PS sample with $M_w = 8.6 \times 10^6$. Thus, for our sample, a value of 85.9 nm for $R_{g,\Theta}$ was obtained from the experimental data $R_{h,\Theta} = 62.7$ nm, and then $R_{g,id}$ with a value of 93.2 nm was calculated from eq 9.

By the definition of $R_{g,id}{}^2 = Na^2/6$ with $N = 7.81 \times 10^4$, the link size a was found to be 8.2×10^{-8} cm for PS. The difference between it and a value of 2.4×10^{-8} cm, which is the contour length of a polymer chain per monomer unit (a_0), reflects the chain rigidity. To treat a macromolecule with a homogeneous persistent chain, the link is related to the persistence length (l) of the chain: $a^2 = a_0(2l)$, where $2l$ is the effective Kuhn length. With $a = 8.2 \times 10^{-8}$ cm and $a_0 = 2.4 \times 10^{-8}$ cm, we got $2l = 28 \times 10^{-8}$ cm or $l = 14$ Å, which was consistent with the theoretical result of $l = 12 \pm 2$ Å.[15]

(iii) The parameter C was evaluated from the chain stiffness parameter. With $\sqrt{C}/a^3 = 0.15$, a value of 6.8×10^{-45} cm^6 was computed for C.

(iv) It is also worthwhile to mention here that the density (ϱ) of dry PS ≈ 1.05 g/mL. Clearly, the density of PS with solvent is less than ϱ (dry PS). The density is usually expressed in terms of n, the number of links per unit volume. With the molecular mass (m) of one PS link of about 104, this corresponds to $n_{dry\,PS} \approx \varrho/104m_p \approx 6.1$ link/nm^3, with m_p being the proton mass.

Note that $1/n_{dry\,PS} = v$ can be considered as an estimate of the value of the excluded volume of one link, and it is usually supposed in the theory that $\sqrt{C} \simeq v$. This is indeed very reasonably obeyed with the numbers given above, because $1/n_{dry\,PS} \approx 0.16$ nm^3 and $\sqrt{C} \approx 0.082$ nm^3.

As to the value of Q (eq 8), an estimate $Q = 0.28$ (mol/g)$^{1/2}$ was found in ref 15. This estimate of $Q = 0.28$ (mol/g)$^{1/2}$ can be represented in a plot of $\alpha_{h,glob}$ [$\equiv(\langle R_h{}^{-1}\rangle/\langle R_{h,id}{}^{-1}\rangle)^{-1}$ versus t_r as shown in Figure 4 of ref 13, and it disagrees with the data of the present work. We therefore reconsider it below.

IV.3. Equilibrium Data. To relate the experimental data of this work to the mean-field theory,[11–15] we consider first the equilibrium data. It is noted that the equilibrium theory has been worked out in many details, while the dynamic theory is incomparably more sketchy.

Following the main idea, we speculate that the final stage of the observed relaxation corresponds to an equilibrium of single chains in the solution. For this state, it was observed that the hydrodynamic radius of the chain $R_h(28\ °C)$ is equal to 19.5 nm.

On the other hand, the ideal coil hydrodynamic radius can be estimated according to the Kirkwood–Riseman theory as $R_{h,id} = [3\sqrt{\pi}/8]R_{g,id}$, yielding $R_{h,id} \approx 63$ nm. The corresponding ratio $\alpha_h = R_h(28\ °C)/R_{h,id} \approx 0.31$ corresponds roughly to the reduced temperature which is less than t_r of -60 (as estimated from curve 1 in Figure 4 of ref 13). With $\tau = (28\ °C - 35\ °C)/(273\ °C + 35\ °C) \approx -0.023$, the value of, say, $t_r \sim -80$ (as estimated from curve 1 in Figure 4 of ref 13) corresponds to a value of $Q \sim 1.1$ (mol/g)$^{1/2}$ which is almost 4 times higher than $Q \sim 0.28$ (mol/g)$^{1/2}$. If we estimate a Q value from the coil-to-globule transition temperature $t_{tr} = -10.2$ for $T = 28.5$ °C ($\tau = -0.021$) for the PS–CYH system,[11] $Q = 0.17$ (mol/g)$^{1/2}$ with $M = 8.12 \times 10^6$. Therefore, we can safely conclude that the previously estimated value of $Q = 0.28$ (mol/g)$^{1/2}$ is too high to fit the present experimental data and curve 1 in Figure 4 of ref 13 should be reconsidered.

If one nevertheless believes the estimate $t_r \simeq -11$ (for $T = 28$ °C) based on Figure 6 of ref 11, then all the other equilibrium quantities can also be found easily. Indeed, the second virial coefficient $|B_{28°}| \sim 0.002$ nm^3 can be found directly from eq 7.

The globule density can be estimated easily by considering the globule as a uniform dense sphere with radius R_h. For a very compact globule we can compute the globule density by first considering a volume occupied by a single coil at the Θ temperature. This volume is then contracted during our quenching process. The difference is on the order of $(1.2)^3 \sim 1.7$. For the sphere with radius R_h, one has $n = N/[(4/3)\pi R_h{}^3] \approx 2.6$ nm^{-3}. Note that $n/n_{dry\,PS}$ $(2.6/6.1) \approx 0.43$, meaning that

the polymer volume fraction inside the globule is, according to our estimates, about 43%.

Note that the ratio $|B_{28°}|/\tau$ is normally supposed to be on the order of the monomer excluded volume. With $|B_{28°}| \sim 0.002$ nm^3, $|B_{28°}|/\tau \approx 0.09$ nm^3 which seems to be a reasonable value in comparison with $v \approx 0.16$ nm^3 taken above from the density of dry PS.

IV.4. Concentration. A very crude estimate of the osmotic virial coefficient of the PS−CYH solution, or of the pairwise globule-to-globule coupling constant, can be done with the data.[11,12] It is seen from Figure 3 in ref 11 that at $t_r \leq -60$, which was estimated based on curve 1 in Figure 4 of ref 13, we have $A_2 \leq -10^{10} R_{g,id}{}^3 \approx -8 \times 10^{15}$ nm^3. In other words, $A_2{}^{chem} = (N_A/M^2)A_2 \leq -7 \times 10^4$ cm^3 mol/g^2. This value of $|A_2{}^{chem}|$ seems unexpectedly large and even counterintuitive. The problem again points toward an overestimate in the magnitude of $Q = 0.28$.

With c expressed in units of the number of links per unit volume and the molecular mass of PS link at 104, 1 link/nm^3 = 0.17 g/mL, so that the estimate based on curve 1 in Figure 4 of ref 13 suggests $c \ll 10^{-32}$ g/mL. Then, the experiments could have been assumed to be performed at incomparably higher concentrations than 10^{-32} g/mL, again due to the overestimate in $Q = 0.28$. In reality, with $t_r \sim -11$ (based on $Q = 0.17$), $c \sim 10^{-6}$ g/mL. Thus, although the value of c is low, it is within the experimentally accessible range. The small c value nevertheless implies an extremely steep drop on the left-hand side of the coexistence curve. Indeed, aggregation of chains has clearly been observed, as it is manifested by the appearance of the second peaks in the insets of Figures 7 and 8.

From Figure 4 in ref 13, the theoretical results indicated that the expansion factor of the hydrodynamic radius of the polymer globule $\alpha_{h,glob} = [R_h{}^{-1}/R_{h,id}{}^{-1}]^{-1} = 0.70$ at $t_r = -11$. Then, $R_h{}^{28°C} = (0.7R_{h,id}) = 43.4$ nm, which is in good agreement with our experimental result of 44.7 nm for the crumpled globule within the experimental error limits. The 44.7-nm value should be the upper bound since a small amount of the aggregates was included in the DLS average hydrodynamic radius measurements.

We conclude that the experiments have been performed with the solution which in thermodynamic terminology should be called the two-phase region with respect to aggregation and phase separation. The experimental results on the crumpled state agree well with theoretical predictions. The question then becomes, what is the characteristic time of this instability development? This question will be addressed in the next sections.

IV.5. Dynamic Data: Single Chain. After an abrupt decrease in temperature from the theta (Θ) condition, the single polymer chain in solution first formed the crumpled globule. The relaxation time τ_{crum} of this process can be written as[22]

$$\tau_{crum} = (\tau_{crum}{}^0/g)(\eta/k_B\Theta)(|B|N^2)(a^6/C) \qquad (10)$$

which is different from eq 6, and the relaxation time of forming a single-chain equilibrium (compact) globule as

$$\tau_{eq} = \tau_{eq}{}^0(\eta/k_B\Theta)(a^6/C)(|B|N^3)[(na^3)^2/N_e] \qquad (11)$$

where η (=0.834 × 10^{-2} P) is the solvent viscosity at 28 °C, k_B (=1.38 × 10^{-6} erg/K) is the Boltzmann constant, N_e is the number of links along a chain between neighboring topological constraints ($N_e = 365$ is an acceptable value for PS), and $\tau_{eq}{}^0$ and $\tau_{crum}{}^0$ are dimensionless coefficients, which are related to experimental conditions. The ratio of the dimensionless coefficients $\tau_{eq}{}^0$ and $\tau_{crum}{}^0$ is expected to be on the order of 1. For simplicity, we define

$$g = \left[1 + \frac{\text{const}\, a^6}{N_e C}\right] \qquad (12)$$

By substituting the values of the parameters as calculated previously, eqs 10 and 11 become

$$\tau_{crum} = 4.43 \times 10^{21}\tau_{crum}{}^0|B| \qquad (13)$$

and

$$\tau_{eq} = 3.45 \times 10^{-18}\tau_{eq}{}^0|B|n^2 \qquad (14)$$

If the ratio of the relaxation times were known, i.e.,

$$\tau_{eq}/\tau_{crum} = 7.79 \times 10^{-40}n^2 \qquad (15)$$

the globule density $n \sim 3.4 \times 10^{19}$ cm^{-3} could be calculated from the ratio of τ_{eq}/τ_{crum} (=323/357) ≃ 0.9.

For the dynamic behavior of a single polymer chain undergoing the coil collapse process, three dynamic quantities were measured experimentally which can be compared with the theoretical predictions. Those are the two relaxation times and the hydrodynamic radius of the kinetic intermediate which we identify with the crumpled globule. We remind the reader that the experimental values are $\tau_{crum} \simeq 357$ s and $\tau_{eq} = 323$ s (as mentioned above, the absolute value of τ depends on the value of $R_h(t\to\infty)$ used, but the ratio of τ's remains a constant no matter what $R_h(t\to\infty)$ was chosen) and $R_{h,crum} = 45$ nm.

To begin with, $R_{h,crum} = 45$ nm and R_h (collapsed globule) ≃ $R_{h,eq} \approx 19.5$ nm yield $g = (R_{h,crum}/R_{h,eq})^3 \approx 12$. If one takes $N_e = 365$, then it means, according to eq 12, const ≈ 93; in other words, the effective relevant value of N_e appears to be N_e/const ≈ 4.

Let us now consider the two characteristic times τ_{crum} and τ_{eq}. Since the viscosity of CYH at 28 °C is equal to $\eta_0 = 0.834 \times 10^{-2}$ P, with $|B_{28°}| \simeq 2.2 \times 10^{-24}$ cm^3, eq 10 yields $\tau_{crum}{}^0 \approx 3.7 \times 10^4$, where the estimate $g \approx 12$ was used and we took $N_e = 365$. The ratio of $\tau_{eq}{}^0/\tau_{crum}{}^0$ is on the order of 1. It is interesting if we take the ratio of $\tau_{crum}/\tau_{crum}{}^0$ and of $\tau_{eq}/\tau_{eq}{}^0$ as normalized characteristic times, which have the values of 9.8 × 10^{-3} and 8.8 × 10^{-3} s, respectively.

We see, therefore, the very good agreement between theoretical and experimental results on the relaxation times. It is understandable that the longest relaxation is indeed associated with reptation, or autoreptation, of the polymer chain through itself. Theoretically, it could be this very process which leads to the formation of knots and, in the compact globular state, to heavily knotted or self-entangled conformations.

On the other hand, we do not have an agreement at all with respect to the shorter relaxation time, with the theoretical value being about 3 orders of magnitude less when compared with the experimental observation. What could be the reason for this dramatic discrepancy? It is, of course, possible that what was observed as a kinetic intermediate is not a crumpled globule. For example, an alternative scenario of the dynamics of coil-to-globule transition could exist (see, for example, ref

23). However, a two-stage kinetics is, in fact, what we have observed. This is why we consider the idea of crumpled (or even sausage) globules as the most plausible explanation. In the framework of this explanation, we remind the reader that the kinetics of the coil collapse in the very early stage, far before the formation of even a crumpled globule, could be given by eq 5.[8] The observed relaxation appeared to have a different exponential character $R_h(t) \sim R_{h,id} \exp(-t/\tau_{crum})$, even though we have missed the first time period due to the time required for thermal equilibration. Nevertheless, we could speculate that even the first stage of the observed relaxation might not be the hydrodynamic collapse as described in refs 8 and 9 but some other process. In view of the fact that the observed values of $\tau_{crum} \approx 357$ s and $\tau_{eq} \approx 323$ s are of the same order of magnitude, it is possible to suggest that even the first of those two relaxation times could somehow be related to entanglements and other topological constraints within the confined volume of the polymer coil which must exhibit a much higher effective viscosity, capable of hindering the localized motions of the segments. It should be emphasized that the existence of even a faster initial stage of relaxation, governed by hydrodynamics and the equation of the type in ref 8, does not contradict the present data set. It cannot be overemphasized that the *actual* viscosity, not the solvent viscosity, should be taken into account in the relaxation process. The much higher viscosity could be the main reason for slowing down the observed processes.

IV.6. Dynamic Data: Aggregation. By quenching from 35 to 28 °C, the experiments were performed at a concentration which was in the metastable region in agreement with the theoretical estimates.[11] It is therefore very important to estimate the characteristic time of the expected development of the instabilities related to aggregation and phase segregation.

According to Smoluchowski, the characteristic time of diffusion-limited aggregation is given by

$$\tau_{aggreg} \simeq \frac{1}{4\pi DRc} \simeq \frac{3}{2c}\frac{\eta}{k_B\Theta} \qquad (16)$$

with c being the concentration (expressed as the number of chains per unit volume) and the diffusion coefficient being given by the Stokes–Einstein equation $D = k_B\Theta/6\pi\eta R_h$. With the numbers cited above, we found $c \approx 6.4 \times 10^{11}$ chains/cm^3 and $\tau_{aggreg} \simeq 0.5$ s, which is surprisingly short when compared with single-chain relaxation times as mentioned and discussed above. This means that throughout the time interval of the order of hundreds of seconds, when appreciable aggregation has not occurred or, better to say, when some considerable fraction of the chains remains segregated, each chain makes thousands of collisions and contacts with other chains. With a very strong tendency toward aggregation in the poor solvent (see A_2 above), what has prevented the polymer chains from aggregation? This interesting question remains unclear.

We have to stress here that this dramatic question is not based on any deep, complicated, and unreliable theory. There is *nothing* theoretical, except the simple relationship[16] from general physics. All the values in eq 16 could be measured directly, and the chains which did not precipitate were directly observed.

V. Coexistence Curve and Coil-to-Globule Transition. It appears that the coil-to-globule transition in the one-phase region of a highly dilute polymer solution has little to do with phase separation; i.e., in extreme dilution, the single-chain globules are far apart from each other with negligible interchain interactions. However, in real experiments, the solution concentration is usually not sufficiently dilute that phase separation could interfere with the coil collapse process, especially when the measurement time becomes long enough. Then, the coil collapse phenomenon is intermixed with the phase separation phenomenon. By taking advantage of the faster intramolecular process in the chain collapse, the two phenomena can be separated by DLS because the aggregates can be much larger than the globules. Nevertheless, the experiment is a delicate balance on the polymer concentration and the solution temperature used.

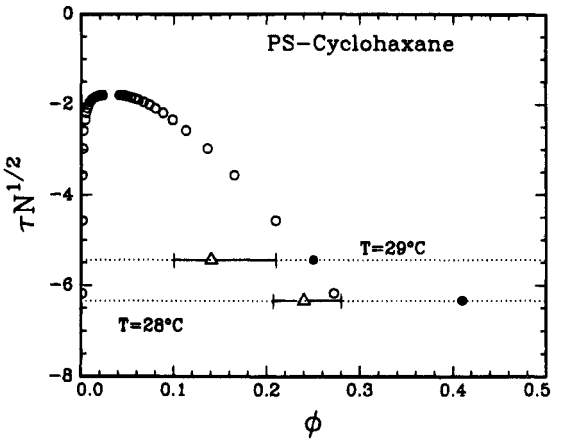

Figure 12. Coexistence (COEX) curve for polystyrene ($M_w = 1.5 \times 10^6$) in cyclohexane. Dotted lines denote $T = 28.0$ °C and $T = 29.0$ °C. Hollow circles denote polymer volume fraction (ϕ) from ref 23; hollow triangles denote ϕ_{comp}; ϕ_{sd} is the corresponding equilibrium polymer volume fraction in the semidilute phase; filled circles denote the polymer volume fraction for the compact globule with $r = R_h$ instead of the Kirkwood–Riseman expression. $\phi_{crum} \simeq 0.02$ with $\phi_{crum} >$ the left side of the COEX curve mainly because of the difference in the PS molecular weight. ϕ_{crum} remains essentially constant because of the steep slope on the left side of the COEX curve.

From the size of the crumpled globule and that of the compact globule, the volume fractions of those globules could be calculated. By assuming that the intraglobular density is uniform and without fluctuation in a sphere of radius r, then $r = 1.2R_h$ for the crumpled globule as given by the Kirkwood–Riseman expression. At a temperature of 28.0 °C for the crumpled globule, the volume of a globule $v_{crum,glob} = (4/3)\pi r^3 = 6.46 \times 10^{-16}$ cm^3 and the volume of a PS chain $v_{PS} = (M/N_A d_{PS}) = 1.35 \times 10^{-1}$ cm^3, where d_{PS} (=1.05 g/mL) is the density of dry polystyrene. Thus, the volume fraction of PS in the crumpled globule $\phi_{crum} \simeq 0.02$. For the compact globule, $\phi_{comp} = 0.24$ where the estimated uncertainties have also been indicated. With $r \simeq R_h$ instead of the Kirkwood–Riseman expression, $\phi_{comp} \simeq 0.41$. We also did DLS measurements at 29.0 °C, where $\phi_{crum} \simeq 0.14$. Interestingly, in comparison with the results measured at 28.0 and 29.0 °C, the difference in the ϕ_{crum} value was small; but the change in ϕ_{comp} was substantial, with $\phi_{comp,29°C} \simeq 0.6\phi_{comp,28°C}$; i.e., the estimated value of ϕ_{crum} was around 0.02, while ϕ_{comp} was in the range of 0.1–0.3 at temperatures between 28.0 and 29.0 °C. The result implies that a single-chain globule contains a large amount of solvent even in its globule state, and the volume fraction of solvent in the compact globule is temperature dependent.

The coexistence curve for PS of $M_w = 1.5 \times 10^6$ is shown in Figure 12, where the y-axis is represented by

Table 1. Comparison of Experimental Results and Parameters Computed from Experimental Data with Grosberg–Kuznetsov Theory

param	exptl results	computed from exptl data	theoretical results
N	7.81×10^4		
t_r	$T = 28.0$ °C	-11.1^a	
$R_{h,\Theta=35°C}$ (nm)	62.7		
$R_{g,\Theta}/R_{h,\Theta}$	1.37[b]		
$R_{g,\Theta}$ (nm)		85.9[c]	
a (cm)		8.2×10^{-8}[d]	
l (Å)		14[e]	12 ± 2[f]
$R_{h,28°C,crum}$ (nm)	44.7		43.4[g]
$R_{h,28°C,comp}$ (nm)	19.5		
N_e/const		~4[h]	$\sim 6 \pm 3$[i]

References, equations and parameters used in the computation: [a] Equation 8 and Figure 6 in ref 11: $t_{tr} = -10.2$; $T = 28.5$ °C; $M = 8.12 \times 10^6$; $Q = 0.17$. [b] Reference 5. [c] $R_{h,\Theta=35°C}$ and $R_{g,\Theta}/R_{h,\Theta}$. [d] $R_{g,\Theta}$, eq 9, and $a = (6/N)^{1/2}R_{g,id}$. [e] $2l = a^2/a_0$; $a_0 = 2.4 \times 10^{-8}$ cm. [f] Reference 15. [g] $\alpha_{h,glob} = 0.7$ at $t_r = -11.1$ from Figure 4 in ref 13. [h] $R_{h,crum}$, $R_{h,comp}$, and eq 12. [i] Reference 22.

a reduced variable $\tau N^{1/2}$ in order to compare the temperature range using PS of two different molecular weights. The hollow circles are the experimental data from ref 29, and the hollow triangles represent ϕ_{comp} at 28 and 29 °C. $\phi_{comp} < \phi_{sd}$ where ϕ_{sd} is the equilibrium volume fraction of PS in the semidilute phase. In comparison with the volume fraction of the PS chain in a single-chain globule at the same temperature, we found $\phi_{crum} < \phi_{comp} < \phi_{sd}$. It is reasonable to predit that when the coil-to-globule transition occured in the two-phase regin, a polymer chain crumpled from a coil and then shrunk to a compact collapsed globule. The polymer concentration in a compacted collapsed globule increased with decreasing size and subsequently reached a certain value, which is still lower than ϕ_{sd}. The globules aggregate with chain interpenetration, and entanglement occurs. Then, the concentration of the polymer-rich phase (very large aggregates) approaches the thermodynamic equilibrium ϕ_{sd} value.

VI. Conclusion

Let us now summarize our main findings. In accordance with the theoretical prediction, the two-stage kinetics of the coil-to-globule transition in the single chain has indeed been observed. All the relevant molecular parameters can be found from the experimental data, and they are summarized in Table 1. We believe that knotting, or topological relaxation, could probably be the main time-consuming stage of single-chain relaxation in a poor solvent.

Let us formulate now the aspects which are unclear and remain a challenge for both theoretical and experimental studies.

(i) The size of the equilibrium compact globule at 28 °C is very small. It leads to a contradiction concerning the value of Q based on the experimental results of the present work and the estimate of Q used in ref 15.

(ii) The shorter of the two observed stages of single-chain collapse may not be simply a hydrodynamically controlled crumpling process, as predicted in ref 8 because of the discrepancy in predicted and observed relaxation times. It is therefore a challenge to understand the nature of the observed first stage of the process and to verify experimentally the existence of the theoretically predicted kinetics[8] on shorter times. Furthermore, the viscosity within the coil must be different from that of the solvent viscosity. This much higher viscosity has to be taken into account in the collapse process.

(iii) Last, but not least, is the question of what could significantly slow down the process of aggregation of chains.

Acknowledgment. B.C. gratefully acknowledges support of this work by the Polymers Program, National Science Foundation (DMR 9301294).

References and Notes

(1) Stockmayer, W. H. *Makromol. Chem.* **1960**, *35*, 54.
(2) Flory, P. J. *Principles of Polymer Chemistry*; Cornell University Press: New York, 1953.
(3) Ptitsyn, O. B.; Kron, A. K.; Eizner, Y. Y. *J. Polym. Sci., Part C* **1968**, *16*, 3509.
(4) Grosberg, A. Y.; Khohklov, A. R. *Soc. Sci. Rev. A: Phys.* **1987**, *8*, 147.
(5) Park, I. H.; Wang, Q.-W.; Chu, B. *Macromolecules* **1987**, *20*, 1965, 2883. Chu, B.; Xu, R.; Zhuo, J. *Macromolecules* **1988**, *21*, 273 and references therein.
(6) Williams, C.; Brochard, F.; Frisch, H. L. *Annu. Rev. Phys. Chem.* **1981**, *32*, 433.
(7) Chan, H. S.; Dill, K. A. *Phys. Today* **1993**, *46*, 24.
(8) de Gennes, P.-G. *J. Phys. Lett.* **1985**, *46*, L-639.3.
(9) Grosberg, A. Yu.; Nechaev, S. K.; Shakhnovich, E. I. *J. Phys. Fr.* **1988**, *49*, 2095.
(10) Yu, J.; Wang, Z.-L.; Chu, B. *Macromolecules* **1992**, *25*, 1618.
(11) Grosberg, A. Yu.; Kuznetsov, D. V. *J. Phys. II Fr.* **1992**, *2*, 1327.
(12) Grosberg, A. Yu.; Kuznetsov, D. V. *Macromolecules* **1992**, *25*, 1970.
(13) Grosberg, A. Yu.; Kuznetsov, D. V. *Macromolecules* **1992**, *25*, 1980.
(14) Grosberg, A. Yu.; Kuznetsov, D. V. *Macromolecules* **1992**, *25*, 1991.
(15) Grosberg, A. Yu.; Kuznetsov, D. V. *Macromolecules* **1992**, *25*, 1996.
(16) Chu, B.; Wang, Z.-L.; Yu, J. *Macromolecules* **1991**, *24*, 6832.
(17) Wang, Z.-L.; Chu, B.; Wang, Q.-W.; Fetters, L. In *New Trends in Physics and Physical Chemistry of Polymers*; Lee, L.-H., Ed.; Plenum Publishing Corp.: New York, 1989.
(18) Chu, B.; Ford, J. R.; Dhadwal, H. S. In *Methods of Enzymology*; Collowick, S., Kaplan, N. O., Eds.; Academic Press: Orlando, FL, 1985; Vol. **117**.
(19) Provencher, S. W. *Makromol. Chem.* **1979**, *180*, 201.
(20) Brown, J. C.; Pusey, P. N. *J. Phys. D* **1974**, *7*, L31.
(21) Chu, B.; Wang, Z.-L. *Macromolecules* **1989**, *22*, 380.
(22) Grosberg, A. Yu.; Kuznetsov, D. V. *Macromolecules* **1993**, *26*, 4249.
(23) Ostrowsky, B.; Bar-Yam, Y. *Europhys. Lett.* **1994**, *25*, 409.
(24) Birshtein, T. M.; Gridnev, V. N.; Skvortsov, A. M. *Mol. Biol. (USSR)* **1981**, *15*, 394.
(25) Chan, H. S.; Dill, K. A. *J. Chem. Phys.* **1993**, *99*, 2116.
(26) Abkevich, V. I.; Gutin, A. M.; Shakhnovich, E. I. *Biochemistry* **1994**, *33*, 10026.
(27) Chan, H. S.; Dill, K. A. *J. Chem. Phys.* **1994**, *100*, 9238.
(28) Pande, V. S.; Grosberg, A. Yu.; Tanaka, T. *J. Chem. Phys.* **1994**, *101*, 8246.
(29) Nakata, M.; Dobashi, T.; Kuwahara, N.; Kaneko, M.; Chu, B. *Phys. Rev. A.* **1978**, *18*, 2683.